Hindawi
Advances in Polymer Technology
Volume 2022, Article ID 8218905, 10 pages
https://doi.org/10.1155/2022/8218905

Research Article

Design and Evaluation of a Cyanate Ester Containing Oxaspirocyclic Structure for Electronic Packaging

Xuefeng Lei, Junxian Ma, Kaiwen Lin, Yuehui Wang, and Zengfang Huang

School of Material Science & Food Engineering, University of Electronic Science and Technology of China, Zhongshan Institute, Zhongshan 528402, China

Correspondence should be addressed to Xuefeng Lei; lxfmd@zsc.edu.cn and Junxian Ma; mjxld@163.com

Received 20 January 2022; Revised 24 April 2022; Accepted 16 May 2022; Published 28 June 2022

Academic Editor: Pierre Verge

A type of pentaerythritol cinnamaldehyde bisphenol dicyanate ester (PCBDCy) containing oxaspirocyclic structure is well designed and synthesized in three steps from cinnamaldehyde, pentaerythritol, phenol, and cyanogen bromide. The products in each step are characterized by elemental analysis, Fourier transform infrared (FT-IR) spectroscopy, and ^{1}H NMR spectroscopy. The mechanical properties, dielectric properties, thermostability, and water absorption of PCBDCy are investigated in detail. The results show that compared with bisphenol A dicyanate (BADCy), the PCBDCy possesses more excellent comprehensive properties. The bending strength and flexural strength are increased by 10.71% and 47.62%, respectively. The fracture toughness K_{IC} and G_{IC} are 1.5 times and 2 times of BADCy, respectively, indicating that its mechanical properties have been considerably improved. The dynamic mechanical curves indicates that the degree of phase separation is significantly reduced, the tan (δ) value representing the flexible phase is obviously shifted to the high temperature region, and the initial decomposition temperature was 12°C higher than that of BADCy, indicating that the material has excellent thermal stability. In addition, the dielectric constant and loss tangent are almost as same as those of BADCy, maintaining good dielectric properties. The water absorption rate has increased to 1.03 ± 0.03%. Compared with BADCy, its comprehensive performance is more suitable for the field of microelectronic packaging.

1. Introduction

Under the background of 5G communication, plastic packaging materials used as electronic components and integrated circuits are called for possessing not only low dielectric constant, dielectric loss, and low moisture absorption but also more excellent flexibility and high-temperature thermal stability to resist the impact of heat and mechanical load generated by high-frequency and ensure the reliability of device operation.

The cyanate ester resin network contains a large number of triazine rings and aromatic rings, which possess the characteristics of a dense arrangement, high symmetry, and high crosslinking. Therefore, the resin has excellent properties, such as a high glass transition temperature (Tg), low dielectric constant, and dielectric loss, as well as dimensional stability. Moreover, ether bonds in the molecular chains and steric effects of the ring structure endow the resin with low moisture absorption. Therefore, cyanate ester resin has been widely studied and applied in multiple areas, such as microwave communication, electronic packaging materials, and PCB substrates.

However, the brittleness of cyanate resin easily causes debonding between the packaging system and functional components, resulting in the failure of the packaging function under variable frequency loading. Thus, the resin should be toughened to meet the requirements of packaging performance, and the components must withstand high-speed and high-frequency conditions. The usual toughening methods are as follows: (1) a copolymerization with thermosetting resins [1–3], (2) a blend of high-temperature-resistant and low-dielectric thermoplastic resins [4–6], (3) the formation of an interpenetrating polymer network (IPN) with a rubber elastomer or block copolymer with linear macromolecules, [7–11], and (4) the introduction of polyhedral oligomeric silsesquioxane

(POSS) or nanoparticles into the system [12–14]. Copolymerization with a thermosetting resin could perform a hybrid homogeneous network resin structure with improved properties but the limited toughening degree. Other toughening methods make the resin exist in a multiphase system, in which thermoplastic resins, rubber elastomers, and linear macromolecular components introduce parts of their chain segments into the network of the cyanate ester resin in block form, improving the yield deformation of the modified system. Thus, the main toughening effect is implemented by plastic deformation, and the plastic phase destroys the phase distribution of the resin network, leading to a decrease in thermal performance.

Based on the unique correlation of the resin structure with its properties, the development of cyanate ester monomers with characteristic properties from molecular design has become an important branch of the cyanate resin research field. This development mainly focuses on improving the thermal properties, dielectric properties, and flame retardancy of the resin. Zhan et al. synthesized an isomeric series of n-propyl-bridged cyanate ester monomers [15]. They reported that when cyanurate oxygen atoms were nearby methyl groups or bridge groups, the resin exhibited a decreased moisture uptake by up to 50%, along with an approximately 20–40°C decrease in the glass transition temperature. They considered that the chemical configuration around reactive groups could substantially modify the properties of the network even when the number density and type of reactive group did not change. Ariraman et al. reported a novel liquid dicyanate ester monomer of 2,2′-bis (4-cyanatophenyl) butane (BBCY) with a low viscosity (~450 mPa·s) at ambient temperature. The cured BBCY resin exhibited a higher Tg, higher initial decomposition temperature, and tensile strength and slightly lower shear strength and impact strength than bisphenol A dicyanate, suggesting that BBCY resin not only had a convenient processing window as a composite matrix but also had excellent physical properties [16]. Chang et al. synthesized a new type of cyanate ester, 1,3-bis(4-cyanatobenzyl) cyclohexane (BCC), which was reinforced by glycidyl silane functionalized mesoporous MCM-41 (FMCM-41) to form cyanate ester nanocomposites. From dielectric studies, it was inferred that a 10 wt. % FMCM-41-reinforced BCC polymer composite exhibited the lowest dielectric constant of 1.98 at 1 MHz [17]. Han et al. reported two kinds of novel phosphinated dicyanate esters, which were copolymerized with the dicyanate ester of bisphenol A (BACY). The results showed that incorporating 1-2 wt. % phosphinated dicyanate esters into BACY enhanced the flame retardancy, dimensional stability, and dielectric properties, exhibiting a small penalty to the thermal properties [18].

As can be seen from the above introduction, from the perspective of molecular design, there are few reports about introducing small flexible structural units into cyanate ester monomer structure for toughening modification. The improvement of modified cyanate esters in one aspect is usually at the cost of the decline of other properties in many reports. In this work, we aim to obtain a kind of cyanate ester resin monomer through introducing oxaspirocycle structure into the monomer molecule, which could increase the distance of triazine rings and the spatial deformation capacity of crosslinked resin, and improve the toughness of cured resin. At the same time, the new cyanate ester resin still keeps high thermal stability and excellent dielectric properties, whose comprehensive performance is superior to BADCy and more suitable for the field of microelectronic packaging.

2. Materials and Methods

2.1. Materials. Cinnamaldehyde (99% purity) was purchased from Wuhan Yancheng Medical Technology Co., Ltd. (Wuhan, China). Pentaerythritol (99% purity) was provided by Guangzhou Bohan Chemical Co., Ltd. (Guangzhou, China). Phosphotungstic heteropoly acid (≥98% purity) was supplied by Zhongshan Jingke Chemical Co., Ltd. (Zhongshan, China). Cyanogen bromide (98% purity) was purchased from Shandong Zibo Qifeng Chuanrun Chemical Co., Ltd. (Zibo, China). Phenol, dimethylbenzene, dichloromethane, anhydrous sodium sulfate, and triethylamine were analytical reagent (AR) grade and supplied by Aladdin Reagent Co., Ltd. (Shanghai, China). Dibutyltin dilaurate (DBTDL, TCI) and p-toluenesulfonic acid (AR) were purchased from Sinopharm Chemical Reagent Co., Ltd. (Shanghai, China). Absolute ethyl alcohol, acetone, and pyridine were all AR grade and purchased from Guangzhou Chemical Reagent Factory (Guangzhou, China). Bisphenol A dicyanate (BADCy) monomer (≥99% purity) was provided by Yangzhou Tianqi New Materials Co., Ltd. (Shanghai, China).

2.2. Equipment and Measurement. FT-IR measurements were performed with a Thermo Nicolet 380 FT-IR spectrometer (America) using 32 scans with a 4 cm^{-1} resolution step in the range of 400-4000 cm^{-1}. The solid sample was mixed with potassium bromide and pressed into a tablet before scanning; the liquid sample was dropwise added onto a potassium bromide tablet and dried for analysis. Elemental analysis was carried out with an Elementar Vario EL III elemental analyser (Germany) to test the contents of C, H, O, and N. ^{1}H-NMR spectra were recorded on a Bruker DRX-400 (Germany) using deuterated acetone as the solvent. Differential scanning calorimeter (DSC) analyses were performed on a TA DSC-25 (America) at a nitrogen flow rate of 50 mL·min^{-1} and a heating rate of 5°C·min^{-1} in a temperature range from 50 to 300°C. The viscosity test was performed with a Yulong NDJ-7 rotary viscometer (China) according to GB/T22235-2008. The mechanical properties were measured according to GB/T2567-2008. Bending strengths were tested using a SANS CMT-6503 desktop electromechanical universal testing machine (China) with a crosshead speed of 2 mm·min^{-1}, and impact strengths were measured using a Liangong JB-300 impact machine tester (China). Dynamic mechanical analyses (DMA) were carried out on a TA DMA850 dynamic mechanical analyser (America) from room temperature to

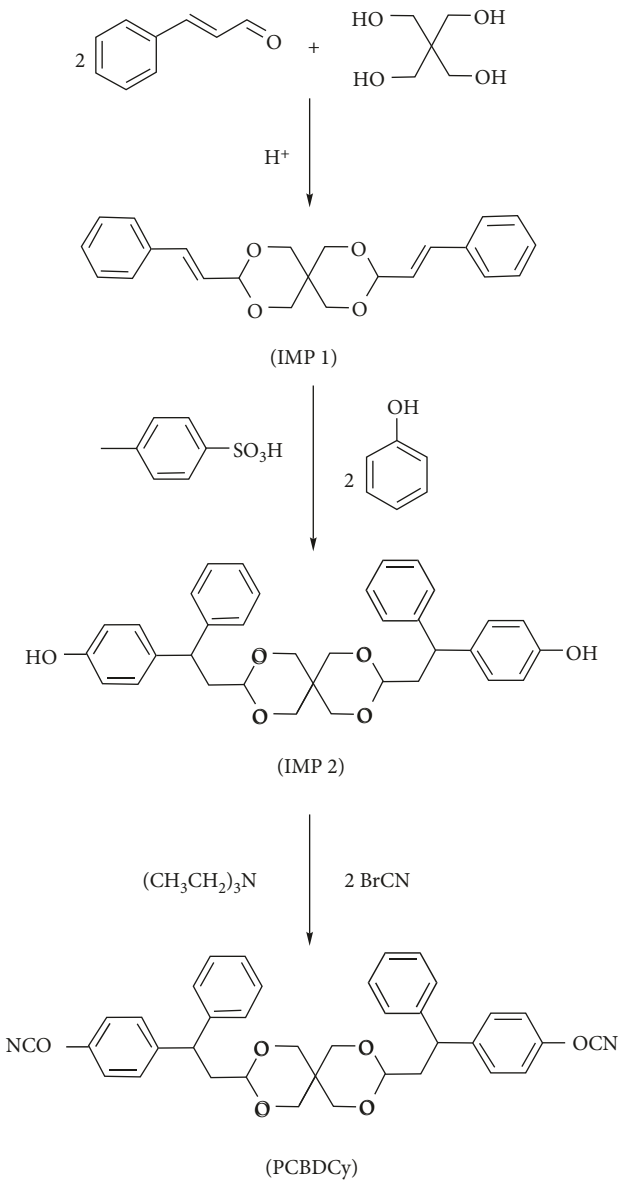

Scheme 1: Synthesis procedure of PCBDCy.

300°C at a frequency of 1 Hz. The sample size was 70 mm × 10 mm × 3 mm. Dielectric properties were determined in a frequency range from 0.1 to 160 MHz at room temperature using a Beijing Guance GCSTD-B dielectric spectrometer (China). The dimension of each sample was Φ25 mm × 3 mm. For the water uptake test, the samples were immersed in boiling water for 48 h, dried with filter paper, and weighed to calculate the water sorption; then, the dielectric properties were tested after immersion. Thermal decomposition properties were measured using a NETZSCH STA 449F3 (Germany) from 25 to 800°C in nitrogen at a heating rate of 10°C·min^{-1}.

2.3. Experimental Principle. The preparation of PCBDCy included three steps: (1) the intermediate product 3,9-distyryl-2,4,8,10-tetraoxa-spiro [5.5] undecane, labeled IMP 1, was synthesized from pentaerythritol and cinnamaldehyde by aldol condensation with a phosphotungstic heteropoly acid (HPWA) catalyst; (2) 3,9-bis(2-(4-hydroxy phenyl) phenethyl)-2,4,8,10-tetraoxa-spiro [5.5] undecane, labeled IMP 2, was prepared by alkylation of IMP 1 with phenol; and (3) IMP 2 was reacted with cyanogen bromide to obtain 3,9-bis(2-(4-cyanatophenyl) phenethyl)-2,4,8,10-tetraoxa-spiro [5.5] undecane (PCBDCy) in the presence of triethylamine as catalyst. The reaction was shown in scheme 1.

2.4. Synthesis

2.4.1. Synthesis of IMP 1. Pentaerythritol (19.58 g) was added into a three-necked flask. And then absolute ethyl alcohol (200 mL) and a certain amount of HPWA (0.5%-1% of the theoretical yield) were added and heated to 60-65°C. Cinnamaldehyde (26.43 g) was added dropwise to the solution under the protection of nitrogen. The mixture was allowed to react at a constant temperature for

Table 1: Elemental analysis of the products.

Sample	C/%	H/%	O%	N/%
IMP 1 ($C_{23}H_{24}O_4$)	75.49	6.717	17.79	—
	(75.80)	(6.638)	(17.56)	—
IMP 2 ($C_{35}H_{36}O_6$)	76.56	6.601	16.84	—
	(76.06)	(6.566)	(17.37)	—
PCBDCy ($C_{37}H_{34}O_6N_2$)	74.12	5.53	15.87	4.48
	(73.75)	(5.65)	(15.95)	(4.65)

(Theoretical values are labeled in parentheses).

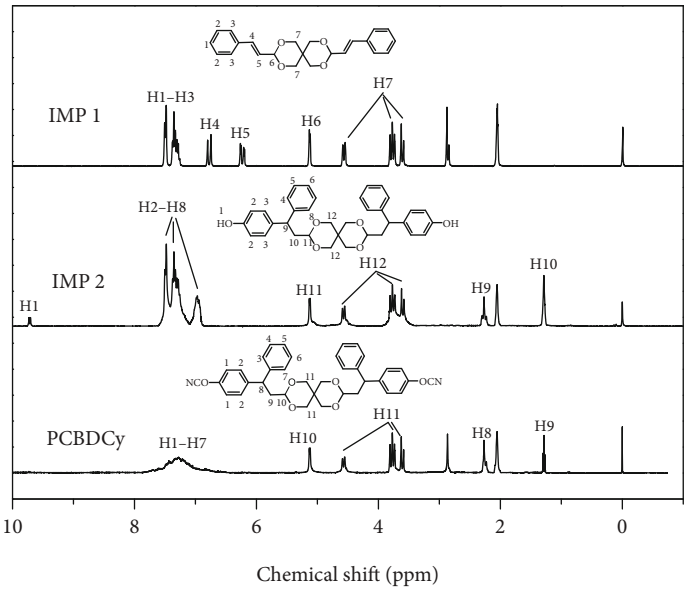

Figure 1: ^{1}H NMR spectra ofIMP1, IMP2, and PCBDCy.

0.5 h and then heated with a reflux temperature of 80°C for 2 h. After the reaction, the temperature was set to below 60°C, and pyridine was added at the equivalence point to neutralize the catalyst. After stirring for 5 min, the solution was filtered to remove HPWA, and then a clear and transparent product solution was obtained. The solution was concentrated and crystallized to obtain white needle-shaped crystals, which were recrystallized from absolute ethyl alcohol. The yield of IMP 1 was 83.57%.

2.4.2. Synthesis of IMP 2. IMP 1 (35.2 g) was added into a 250 mL three-necked flask, and then dimethylbenzene solvent (200 mL) and a certain amount of p-toluenesulfonic acid (0.5%-1% of the theoretical yield) were added as catalysts. The mixture was heated to 80-85°C, and phenol (37.64 g) was added dropwise into the mixture under the protection of nitrogen. Subsequently, the reaction was kept for 0.5 h at the above temperature and then at a reflux temperature of 143°C for 4 h. After the reaction, the mixture was cooled to 85°C, repeatedly washed with hot water (85°C), placed in a separatory funnel, and allowed to stand overnight for stratification. The upper dimethylbenzene solution was collected and dried by sodium sulfate and then distilled at a reduced pressure in the temperature range of 130-170°C to obtain a brownish black and viscous product (IMP 2, yield: 72.35%). The product was diluted to 40% solution with acetone for the next synthesis procedure.

2.4.3. Synthesis of PCBDCy. A acetone solution of IMP 2 (151.5 g, 0.1 mol IMP 2) and 400 mL of dichloromethane were added into a 1000 mL four-necked flask with an electric stirrer, a thermometer, and a protective nitrogen device; next, the mixture was stirred for 20 min in an ice salt bath (-20~ -10°C). Then, cyanogen bromide (22.77 g, 0.215 mol) was added into the flask and stirred until evenly dispersed. After that, triethylamine (23.27 g, 0.23 mol) was slowly added dropwise into the system in an atmosphere of nitrogen and reacted for 3 h at -10~ -8°C. After the reaction, the mixture was repeatedly washed and extracted 5 times using aqueous alkali in ice (0.5 mol/L) and ice water in turn. Then, the dark brown dichloromethane layer was separated and dried by an adequate amount of anhydrous sodium sulfate.

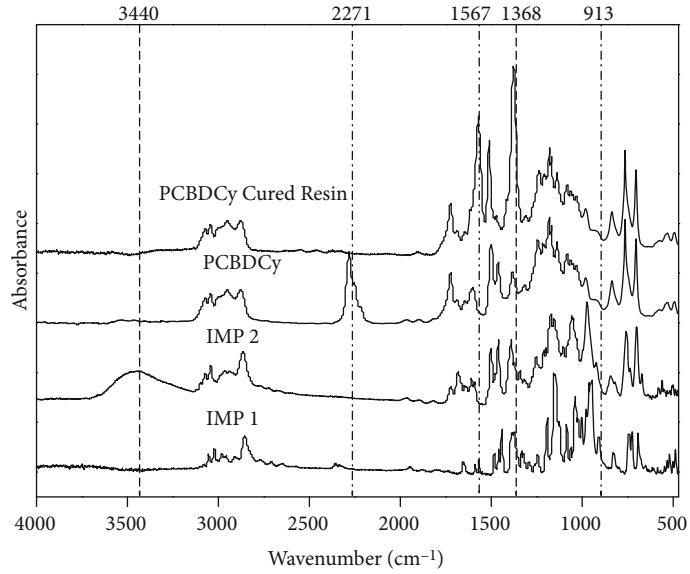

Figure 2: FT-IR spectra of IMP1, IMP2, PCBDCy, and the cured resin.

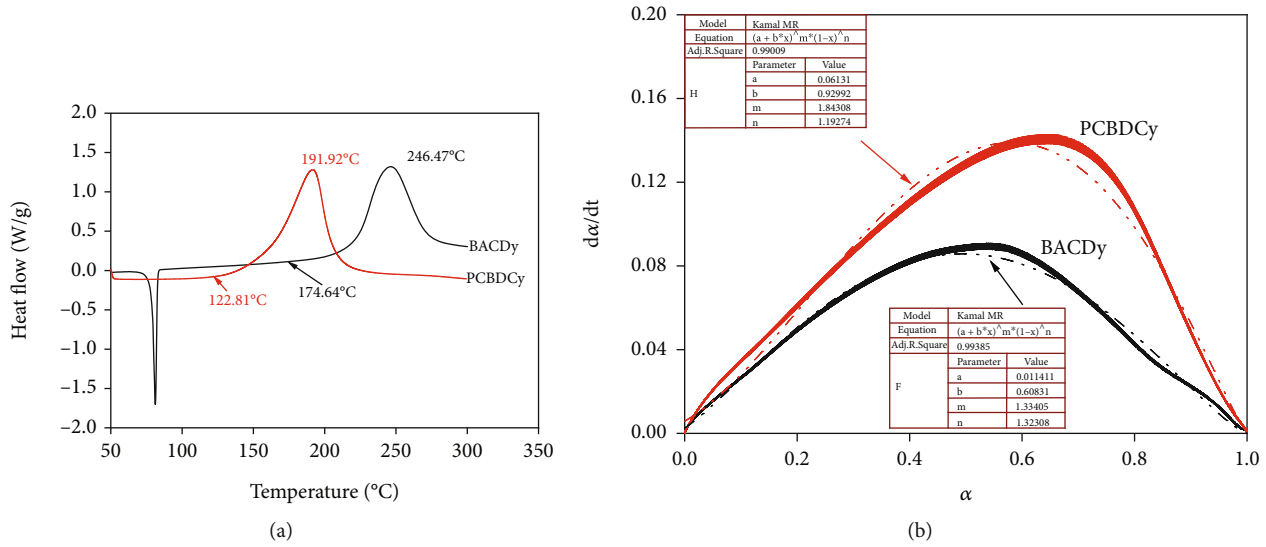

Figure 3: DSC curves and simulations of the nonisothermal curing reaction of PCBDCy and BADCy.

After standing for overnight, the mixture was filtered and transferred into a rotary evaporator to remove dichloromethane by reduced pressure distillation. Next, brown and transparent PCBDCy was obtained (yield: 64.17%), which was prepared in an 80% acetone solution for later use.

2.4.4. Synthesis of Cured PCBDCy. A certain amount of the PCBDCy acetone solution was placed in a 250 mL three-necked flask and heated to 60°C under reflux in an air atmosphere with electric stirring. Then, 0.02 wt. % DBTDL (calculated by the weight of PCBDCy) was added into the flask. A transparent brown color solution was obtained after 10 min of constant stirring. Some of the solution was transferred to a PE pipe and diluted to a 20% acetone solution for DSC and FT-IR tests. The rest of solution was poured into a preheated PTFE mould and cured according to the following procedure: 90°C for 2 h, 120°C for 1 h, 130°C for 2 h, 150°C for 2 h, 180°C for 3 h, and 200°C for 1 h. The cured samples were demoulded, cut, and polished for performance tests.

3. Results and Discussion

3.1. Characterization of Products

3.1.1. Elemental Data. The elemental analysis data of IMP 1, IMP 2, and PCBDCy were shown in Table 1. The test values

Table 2: Mechanical and water absorption properties of cured PCBDCy and BADCy.

Properties		PCBDCy	BADCy
Bending properties	Bending strength (MPa)	62 ± 2	56 ± 1
	Bending modulus (MPa)	1755 ± 100	2531 ± 200
Fracture toughness	K_{IC} (MPa·m$^{1/2}$)	1.2 ± 0.1	0.8 ± 0.1
	G_{IC} (kJ·m^{-2})	236 ± 30	117 ± 20
Tensile properties	Tensile strength (MPa)	31 ± 2	21 ± 1
	Tensile modulus (MPa)	1071 ± 100	1161 ± 100
	Breaking elongation (%)	3.0 ± 0.1	2.2 ± 0.1
Water absorption (%)		1.03 ± 0.03	0.67 ± 0.02

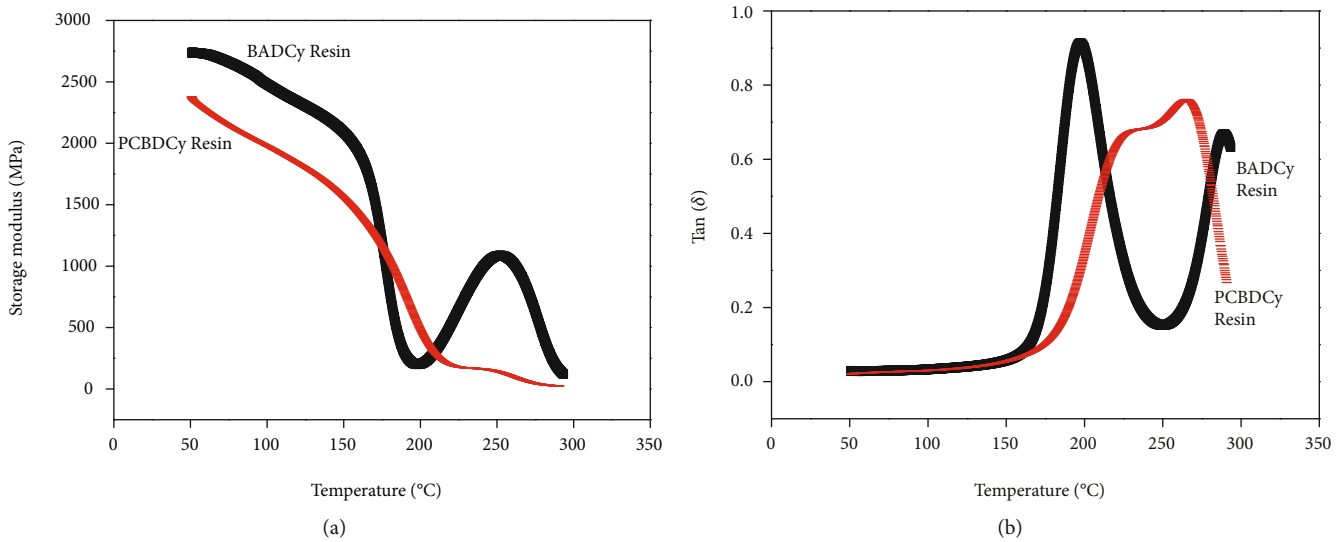

Figure 4: Storage modulus (a) and tan delta (b) of cured PCBDCy and BADCy.

basically coincided with the theoretical values, indicating the formation of intermediate and target products.

3.1.2. ^{1}H-NMR Spectra. ^{1}H-NMR spectra of IMP 1, IMP 2, and PCBDCy were shown in Figure 1.

In the spectrum of IMP 1, protons on benzene rings appeared in the range of 7.51-7.26 ppm (H_1-H_3), and alkene protons were observed at 6.80-6.75 ppm (H_4) and 6.26-6.19 ppm (H_5), respectively [19, 20]. Peaks observed at 5.13-5.12 ppm were attributed to acetal protons (H_6). The eight methylene protons (H_7) from pentaerythritol were split into multiple peaks because of the effect of the chiral axis [21]. In the spectrum of IMP 2, hydroxyl protons (H_1) were detected at 9.74 ppm [22]. At the same time, alkene proton signals disappeared, while methine and methylene protons were observed at 2.23 ppm (H_9) and 1.28 ppm (H_{10}), respectively [23]. The signal range of aromatic protons was widened to reach the high field due to the presence of phenol rings in the structure. In the spectrum of PCBDCy, the signal of hydroxyl protons disappeared, and the signal of protons on aromatic rings became wider. The other signal patterns were basically the same as IMP2.

3.1.3. FT-IR Spectra. FT-IR spectra of the products were shown in Figure 2. In the spectrum of IMP 1, the –C=O absorption peak of cinnamaldehyde at approximately 1719 cm^{-1} disappeared, indicating the aldol condensation reaction occurred. Compared with that of IMP 1, the stretching vibrations of the –C=C– group disappeared for IMP 2; at the same time, a strong and wide –OH absorption peak at approximately 3440 cm^{-1} appeared, indicating the formation of IMP 2.

In the spectrum of PCBDCy, the –C≡N characteristic absorption peak of the –OCN functional group was observed at 2271 cm^{-1}, and –C–O– absorption peaks appeared at 1244 cm^{-1} and 1061 cm^{-1}, respectively. The intensity of the absorption band of –OH from IMP 2 at 3440 cm^{-1} weakened to almost disappearing, demonstrating that PCBDCy was formed but that a trace amount of phenol may still present. Moreover, absorption peaks at 1714 cm^{-1}, 1567 cm^{-1}, and 1378 cm^{-1} could be observed, which represented the –C=O (the result of rearrangement), –N=C–O–, and –O– groups from the triazine ring, respectively, indicating that a small amount of PCBDCy was polymerized in the product.

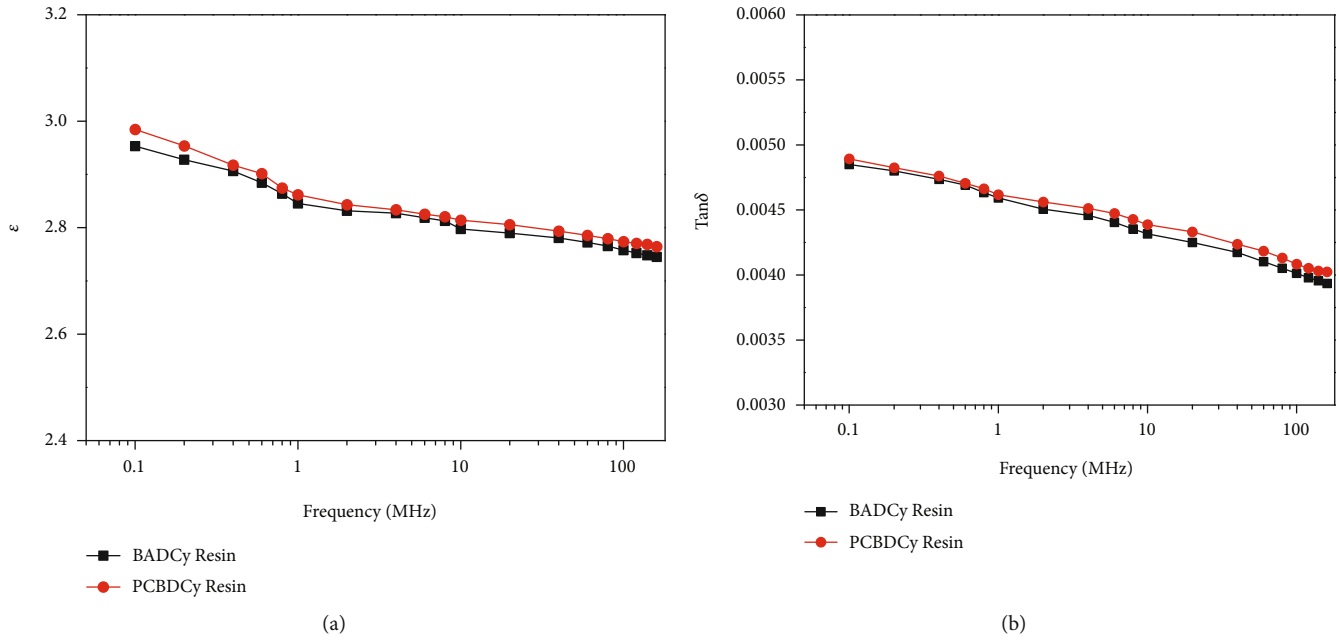

Figure 5: Dielectric constants (a) and dielectric loss tangents (b) of cured PCBDCy and BADCy.

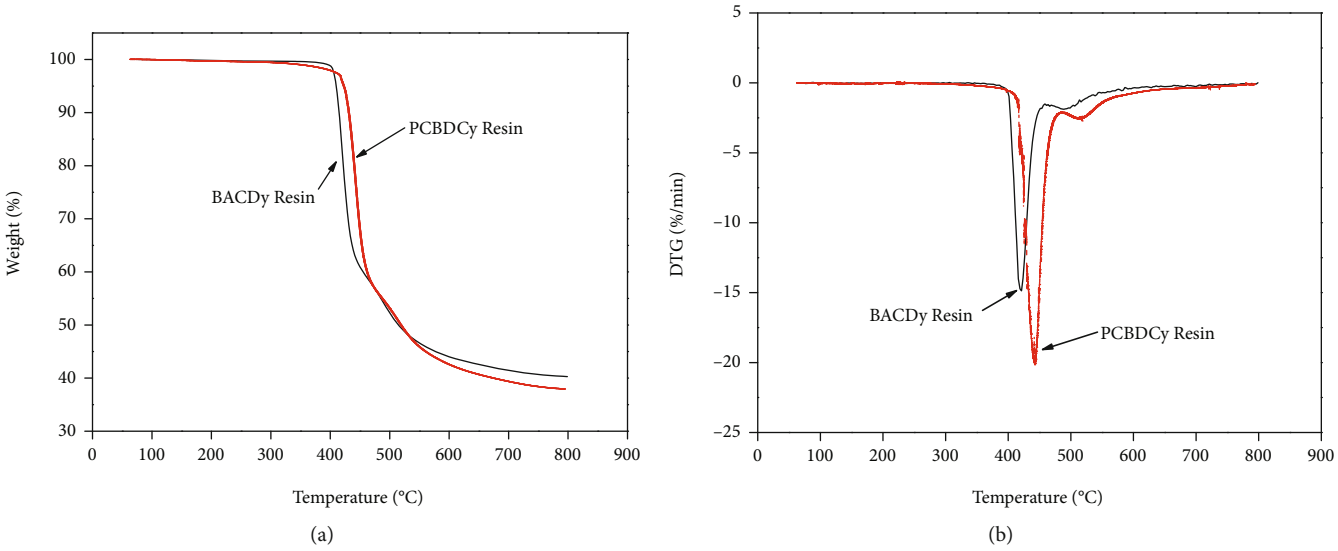

Figure 6: TG (a) and DTG (b) curves of cured PCBDCy and BADCy.

3.2. Properties of PCBDCy

3.2.1. Physical and Chemical Properties. The obtained PCBDCy was transparent and brown color liquid. Its viscosity was about 2500~3000 mPa·s, and the –OCN content was 12.85 ± 1%.

3.2.2. Curing Behaviors of PCBDCy. In the FT-IR spectrum of cured PCBDCy (seen in Figure 2), the–C ≡ N absorption peak at 2271 cm^{-1} absolutely disappeared after the curing procedure, and the stretching vibrations of –N=C–O– and –O– groups were distinctly enhanced, which illustrated that PCBDCy monomers were completely self-crosslinked ,and that a crosslinked network based on triazine rings was formed in the cured product. In addition, the –OH absorption peak at approximately 3440 cm^{-1} disappeared completely, indicating that phenol was involved in the curing reaction.

Figure 3(a) shows the nonisothermal DSC curves of PCBDCy and BADCy. The DSC curve of PCBDCy had no endothermic melting peak, and its onset and peak temperatures of the exothermic curing reaction were observed at 122.81°C and 191.92°C, respectively. Compared with those of BADCy, the temperatures were separately reduced by 51.83°C and 54.55°C. The curing reaction of PCBDCy moved to the low-temperature area, indicating that

PCBDCy could crosslink and form a curing network at low temperatures. The reason may be that the oxaspirocycle in PCBDCy molecules increased the distance between aromatic rings connected with the –OCN group; therefore, the effects of steric hindrance were reduced when triazine rings were formed.

Figure 3(b) simulates the dynamic scanning DSC curves of the curing reactions of BADCy and PCBDCy on the basis of the self-catalytic kinetic model [24, 25]. The results indicated that PCBDCy had a curing behavior similar to that of BADCy, while still complying with the self-catalytic kinetic model. Compared with that of BADCy, the maximum curing reaction rate of PCBDCy appeared at a higher conversion region, indicating that PCBDCy had more self-catalytic trend; hence, the exothermic curing process of PCBDCy was shorter than that of BADCy as shown in the DSC curve.

3.2.3. Mechanical and Water Absorption Properties. A comparison of the mechanical and water absorption properties of PCBDCy and BADCy was shown in Table 2.

It was found that the bending strength, fracture toughness, tensile strength, and breaking elongation of PCBDCy were significantly higher than those of BADCy, illustrating the improvement in toughness. However, the water absorption property showed a slight increase. The improvement in the mechanical performance of PCBDCy was related to its structure. The PCBDCy monomer contained oxaspirocyclic groups, and the flexibility of these chain segments gave the cured resin a stronger yield deformation capacity when resisting external forces. In addition, these flexible segments replaced the branched carbon chain in BADCy, which increased the distance between triazine rings, reduced the crosslinking density, enlarged the deformation space in the network, strengthened the deformation ability, and improved the toughness of the resin. As a result, the flexural strength, fracture toughness, and tensile strength of PCBDCy increased. However, due to the introduction of the polar group –O–, the water absorption rate of the resin increased.

3.2.4. Dynamic Mechanic Properties. The dynamic mechanics performances of cured PCBDCy and BADCy were shown in Figure 4.

In Figure 4(a), the storage modulus of BADCy decreased with an increasing temperature when it was below 150°C. In the middle temperature range (150-250°C), the modulus decreased sharply at the beginning which was even lower than that of PCBDCy at the temperature of 176-210°C and then showed an increasing trend. After 250°C, the modulus continued to decrease. By comparison, the storage modulus of PCBDCy was lower than that of BADCy, which gradually reduced with the increasing temperature. And the modulus had no obvious changes in the high-temperature area.

In the BACDy resin network structure, there were short alkane chain segments with symmetrical side methyl group and a small amount of byproduct for linear macromolecular, which possessed relatively large rotation flexibility. So, the movement abilities as well as the thawing ability to glass state of the resin were strengthened with heating temperature increasing. But the short alkane units caused close distance between triazine rings and high crosslinking density, the chain segments movement and the thawing ability were hindered because of the high crosslinking structure. The two opposing effects led to the result that the storage modulus of BADCy decreased first and then increased in the middle temperature region. By comparison, the triazine rings were connected with long oxaspirocyclic groups in the PCBDCy network. Although its flexibility was lower than the short alkane chain, the chain segment was longer; so, the distance between triazine rings was enlarged, and the crosslinking density was smaller. And the hindering effect on segmental motion was decreased as well as the thawing ability. Therefore, the storage modulus of PCBDCy decreased with the increasing temperature.

In Figure 4(b), the loss modulus of BACDy resin was divided into two stages taking 250°C as demarcation point. The first stage represented the glass-thawing process of the short flexible alkane chain segment with symmetrical methyl group, and the glass transition temperature occurred at 197°C. The second stage represented the glass-thawing process of rigid triazine rings, with glass transition temperature at 289°C. The results showed that BACDy resin network performed multiphase and the phase separation with the increase of temperature [26–28]. The curve of PCBDCy resin, by contrast, had no obvious temperature partition between the glass-thawing process of flexible oxaspirocyclic chain segment and the rigid triazine ring units with the increase of temperature, and the curve showed glass transition at 265.33°C with a shoulder peak of glass transition at 233.12°C. The results showed that the network of PCBDCy resin was still multiphase, but the degree of phase separation was weakened with the change of temperature.

3.2.5. Dielectric Properties. Figure 5(a) shows the variation of dielectric constant with different frequencies at room temperature for PCBDCy and BADCy. It can be seen from the figure that the dielectric constants decrease obviously at a lower frequency region and then almost keep constant at higher frequency. The decrease in dielectric constant with an increase in frequency may be attributed to the electrical relaxation processes as a result of lagging in dipole orientation polarization [29]. The PCBDCy shows slightly higher dielectric constant than BADCy. This may be because the presence of oxaspirocyclic segments increase the polarization in an electric field, but the PCBDCy molecule is symmetrical; so, the dielectric constant increases not much.

Figure 5(b) displays the variation of dielectric loss with frequencies for PCBDCy and BADCy. Dielectric loss is the function of the relaxation process which depends on the change in the viscoelastic nature of the polymer [30, 31]. In the structure of PCBDCy, oxaspirocyclic segments decreased the crosslinking density, endowing the molecules with more flexibility and deformability, thus the activity of the chain segment increases, and the orientation of polar groups is less constrained by the chain segment, leading to

an increasing dielectric loss. On the other hand, the existence of oxaspirocycles and the increased number of aromatic rings restrict the free rotation of valence bonds and the flexible curling of molecules to a certain degree; so, the extent of an increase in the dielectric loss tangent is very small.

3.2.6. Thermal Decomposition. The comparison of the TG and DTG curves between PCBDCy and BADCy is displayed in Figure 6. The results show that both PCBDCy and BADCy decompose in two stages. The initial decomposition temperature (T5%) of BADCy is 410°C, and the maximum thermal decomposition rates of the two stages appear at 421°C and 489°C. The carbon residue rate is 40.33%. In comparison, the T5% of PCBDCy is 422°C, the two maximum thermal decomposition rates separately increase to 442°C and 518°C, and the carbon residue rate decreases to 37.95%. The above changes are also related to the introduction of oxaspirocycles and aromatic rings.

4. Conclusion

Considering the relationship between structure and properties, a constitutional unit of oxaspirocycle was introduced to the cyanate monomer to prepare a pentaerythritol cinnamaldehyde bisphenol dicyanate ester. The intermediate and final products were characterized and confirmed the final product of 3,9-bis(2-(4-cyanatophenyl) phenethyl)-2,4,8,10-tetraoxa-spiro [5.5] undecane (PCBDCy). The curing kinetic behavior of PCBDCy was proven to obey the self-catalytic kinetic model, and the self-catalysis process appeared even more obvious than that of bisphenol A dicyanate (BADCy); the crosslinking temperature of PCBDCy was markedly lowered. Compared with those of BACDy resin, the bending strength, fracture toughness, tensile strength, and breaking elongation of the PCBDCy resin were significantly improved. The bending strength reached 62 ± 2 MPa, the fracture toughness of K_{IC} was $1.2 \pm 0.1\ \mathrm{MPa \cdot m^{1/2}}$, and G_{IC} was $236 \pm 30\ \mathrm{kJ \cdot m^{-2}}$. Although the temperature resistance performance decreased, the Tg value still reached 265.33°C. In addition, the water absorption of PCBDCy was $1.03 \pm 0.03\%$, and ε and tan δ at 1 MHz were 2.86 and 0.00462 with slight decreases. The initial decomposition temperature (T5%) increased, and the decomposition process moved to higher temperatures.

Data Availability

All the data used to support the findings of this study are included within the article.

Conflicts of Interest

The authors declare that they have no conflicts of interest.

Authors' Contributions

Junxian Ma and Xuefeng Lei are co-first authors.

Acknowledgments

This work was supported by grants from the Zhongshan Major Science and Technology Specific Projects (No. 2019B2017), Zhongshan Science and Technology of Social Public Welfare Program (No. 200904143645459), Guangdong Provincial Colleges and Universities Characteristic Innovation Project (No. 2020KTSCX179), and Innovation Team of Colleges and Universities in Guangdong Province (2020KCXTD030).

Supplementary Materials

Graphic abstract synthesis and properties of a pentaerythritol cinnamaldehyde bisphenol dicyanate ester Xuefeng Lei[#], Junxian Ma[#,]*, Kaiwen Lin, Yuehui Wang, and Zengfang Huang. A new pentaerythritol cinnamaldehyde bisphenol dicyanate ester (PCBDCy) aimed to toughness is well designed and investigated in detail. The researches focus on its mechanical properties, dielectric properties, thermostability, and water absorption. It is proved that the overall performance of PCBDCy is superior to that of bisphenol A dicyanate (BADCy). *(Supplementary Materials)*

References

[1] I. Harismendy, M. D. Rio, A. Eceiza, J. Gavalda, C. M. Gomez, and I. Mondragon, "Morphology and thermal behavior of dicyanate ester-polyetherimide semi-IPNS cured at different conditions," *Journal of Applied Polymer Science*, vol. 76, no. 7, pp. 1037–1047, 2000.

[2] J. W. Hwang, K. Cho, T. H. Yoon, and C. E. Park, "Effects of molecular weight of polysulfone on phase separation behavior for cyanate ester/polysulfone blends," *Journal of Applied Polymer Science*, vol. 77, no. 4, pp. 921–927, 2000.

[3] F. Wu, C. C. Tuan, B. Song, K. S. Moon, and C. P. Wong, "Controlled synthesis and evaluation of cyanate ester/epoxy copolymer system for high temperature molding compounds," *Journal of Polymer Science Part A: Polymer Chemistry*, vol. 56, no. 13, pp. 1337–1345, 2018.

[4] C. Uhlig, M. Bauer, J. Bauer, O. Kahle, A. C. Taylor, and A. J. Kinloch, "Influence of backbone structure, conversion and phenolic co-curing of cyanate esters on side relaxations, fracture toughness, flammability properties and water uptake and toughening with low molecular weight polyethersulphones," *Reactive and Functional Polymers*, vol. 129, pp. 2–22, 2018.

[5] A. Inamdar, J. Cherukattu, A. Anand, and B. Kandasubramanian, "Thermoplastic-toughened high-temperature cyanate esters and their application in advanced composites," *Industrial and Engineering Chemistry Research*, vol. 57, no. 13, pp. 4479–4504, 2018.

[6] Q. S. Tao, W. J. Gan, Y. F. Yu, M. H. Wang, X. L. Tang, and S. J. Li, "Viscoelastic effects on the phase separation in thermoplastics modified cyanate ester resin," *Polymer*, vol. 45, no. 10, pp. 3505–3510, 2004.

[7] Z. H. Li, J. K. Hu, L. Ma, and H. X. Liu, "High glass transition temperature shape-memory materials: Hydroxyl-terminated polydimethylsiloxane-modified cyanate ester," *Journal of Applied Polymer Science*, vol. 137, p. 48765, 2019.

[8] L. Zhai, Z. X. Liu, C. Li et al., "Cyanate ester resin based composites with high toughness and thermal conductivity," *RSC Advances*, vol. 9, no. 10, pp. 5722–5730, 2019.

[9] M. C. Cai, Q. L. Yuan, and F. R. Huang, "Catalytic effect of poly (silicon-containing arylacetylene) with terminal acetylene on the curing reaction and properties of a bisphenol A type cyanate ester," *Polymer International*, vol. 67, no. 11, pp. 1563–1571, 2018.

[10] J. X. Ma, X. F. Lei, Y. H. Wang, and Y. Y. Sun, "Toughening modification of cyanate ester with amino-terminated polyoxypropylene," *Iranian Polymer Journal*, vol. 27, no. 3, pp. 145–151, 2018.

[11] L. Tang, J. L. Zhang, Y. S. Tang et al., "Compos," *Part B-Engineering*, vol. 186, pp. 1–8, 2020.

[12] V. Bershtein, A. Fainleib, P. Yakushev et al., "High performance multi-functional cyanate ester oligomer-based network and epoxy-POSS containing nanocomposites: Structure, dynamics, and properties," *Polymer Composites*, vol. 41, no. 5, pp. 1900–1912, 2020.

[13] A. Fainleib, K. Gusakova, O. Grigoryeva, O. Starostenko, and D. Grande, "Synthesis, morphology, and thermal stability of nanoporous cyanate ester resins obtained upon controlled monomer conversion," *European Polymer Journal*, vol. 73, pp. 94–104, 2015.

[14] K. W. Liang, G. Z. Li, H. Toghiani, J. H. Koo, and C. U. Pittman, "Cyanate ester/polyhedral oligomeric silsesquioxane (POSS) nanocomposites: synthesis and characterization," *Chemistry of Materials*, vol. 18, no. 2, pp. 301–312, 2006.

[15] A. J. Guenthner, B. G. Harvey, A. P. Chafin et al., "Effect of segmental configuration on properties ofn-propyl-bridged polycyanurate networks," *Macromolecules*, vol. 50, no. 13, pp. 4887–4896, 2017.

[16] X. B. Zhan, L. L. Wang, J. Y. Zhang, and J. Cheng, "Synthesis, properties and cure chemistry of a novel room-temperature liquid cyanate ester," *Materials & Design*, vol. 88, pp. 1100–1108, 2015.

[17] M. Ariraman, R. S. Kumar, and M. Alagar, "Studies on FMCM-41 reinforced cyanate ester nanocomposites for low k applications," *RSC Advances*, vol. 4, no. 101, pp. 57759–57767, 2014.

[18] H. C. Chang, H. T. Lin, and C. H. Lin, "Benzoxazine-based phosphinated bisphenols and their application in preparing flame-retardant, low dielectric cyanate ester thermosets," *Polymer Chemistry*, vol. 3, no. 4, pp. 970–978, 2012.

[19] Y. Han, D. H. Tang, G. X. Wang et al., "Phthalonitrile resins derived from vanillin: synthesis, curing behavior, and thermal properties," *Journal of Polymer Science*, vol. 38, no. 1, pp. 72–83, 2020.

[20] L. P. Sheng, J. C. Zeng, S. L. Xing et al., "A new resin with improved processability and thermal stability," *High Performance Polymers*, vol. 29, no. 1, pp. 13–25, 2017.

[21] R. B. Wei, J. Zhang, S. Z. Chen, and Y. Liang, "Synthesis and structure characterization of poly-acetal-spiro-vic-diether," *Chinese Journal of Organic Chemistry*, vol. 25, pp. 116–119, 2005.

[22] T. Wang, A. Q. Dayo, Z. L. Wang et al., "Novel self-promoted phthalonitrile monomer with siloxane segments: synthesis, curing kinetics, and thermal properties," *New Journal of Chemistry*, vol. 46, no. 9, pp. 4072–4081, 2022.

[23] H. X. Zhu, Y. Liu, Y. X. Wu, J. J. Qiu, and C. M. Liu, "Unique self-catalyzed bio-benzoxazine derived from novel renewable acid-containing diamines based on levulinic acid and furfurylamine: Synthesis, curing behaviors and properties," *Reactive and Functional Polymers*, vol. 155, p. 104716, 2020.

[24] S. Hao, J. X. Zhang, X. M. Yang, T. C. Li, and H. Z. Song, "A novel strategy for fabricating highly stretchable and highly conductive photoluminescent ionogelsviaanin situself-catalytic cross-linking reaction in ionic liquids," *Journal of Materials Chemistry C*, vol. 9, no. 17, pp. 5789–5799, 2021.

[25] A. I. Olamilekan and H. Yeo, "Curing behavior of 4,4'-diglycidyloxybiphenyl with p-phenylene diamine derivatives," *Macromolecular Research*, vol. 28, no. 10, pp. 960–967, 2020.

[26] Q. B. Guan, L. Yuan, Y. Zhang, A. J. Gu, and G. Z. Liang, "Improving the mechanical, thermal, dielectric and flame retardancy properties of cyanate ester with the encapsulated epoxy resin-penetrated aligned carbon nanotube bundle," *Composites Part B: Engineering*, vol. 123, pp. 81–91, 2017.

[27] L. Yuan, S. D. Huang, A. J. Gu et al., "A cyanate ester/microcapsule system with low cure temperature and self-healing capacity," *Composites Science and Technology*, vol. 87, pp. 111–117, 2013.

[28] K. S. S. Kumar, C. P. R. Nair, and K. N. Ninan, "Investigations on the cure chemistry and polymer properties of benzoxazine–cyanate ester blends," *European Polymer Journal*, vol. 45, no. 2, pp. 494–502, 2009.

[29] A. Nihmath and M. T. Ramesan, "Fabrication, characterization, dielectric properties, thermal stability, flame retardancy and transport behavior of chlorinated nitrile rubber/hydroxyapatite nanocomposites," *Polymer Bulletin*, vol. 78, no. 12, pp. 6999–7018, 2021.

[30] K. Suhailath, M. Thomas, and M. T. Ramesan, "Studies on mechanical properties, dielectric behavior and DC conductivity of neodymium oxide/poly (butyl methacrylate) nanocomposites," *Polymers and Polymer Composites*, vol. 29, no. 8, pp. 1200–1211, 2021.

[31] A. Nihmath and M. T. Ramesan, "Comparative evaluation of oil resistance, dielectric properties, AC conductivity, and transport properties of nitrile rubber and chlorinated nitrile rubber," *Progress in Rubber, Plastics and Recycling Technology*, vol. 37, pp. 131–147, 2021.